Available online at www.sciencedirect.com
SCIENCE DIRECT®
Journal of Magnetic Resonance 171 (2004) 330–337
JMR Journal of Magnetic Resonance
www.elsevier.com/locate/jmr

Product operator analysis of the influence of chemical exchange on relaxation rates

Djaudat Idiyatullin*, Shalom Michaeli, Michael Garwood

Center for Magnetic Resonance Research, Department of Radiology, University of Minnesota Medical School, Minneapolis, Minnesota, United States

Received 11 May 2004; revised 14 September 2004
Available online 13 October 2004

Abstract

Measurements of chemical-exchange processes by NMR are widely used to obtain valuable information about molecular dynamics and structure. Here, a computational method is introduced to assess the influence of chemical exchange on spin relaxation rates. The method is based on the inclusion of a random exchange process in product operator calculations on a microscopic level. This product operator approach can be applied to estimate exchange contributions when using sophisticated pulse sequences that cannot be easily described analytically. The method applies to the full range of exchange times measurable by NMR and can incorporate interference effects between exchange and other processes such as scalar coupling. To demonstrate its utility, simulated relaxation data were compared with theoretical predictions of spin-locking and Carr-Purcell spin-echo sequences with hard and adiabatic pulses, using different time scales for a two-site chemical-exchange process. Finally, simulations were used to examine a system in which a second random process is superimposed on a simple two-site exchange process. The method was found to provide a simple and robust tool to analyze pulse sequences and equations commonly used to study exchange-induced relaxation.

Keywords: Chemical-exchange; NMR relaxation; CPMG; Spin-lock; Simulation; Bloch-McConnell equations; Product operator; Density matrix; Random process; Adiabatic pulses

1. Introduction

Chemical and physical processes causing perturbation of the magnetic environment of atoms are usually referred to as "chemical exchange." The time scales of many biologically important processes fall in the microsecond-millisecond range, making NMR a powerful tool to study these processes [1]. Chemical-exchange processes can be assessed from measurements of spin relaxation rates. In such applications, common approaches include the determination of the transverse relaxation rate constant (R_2) using a Carr-Purcell-Meiboom-Gill (CPMG) technique [2,3] and the spin–lattice relaxation rate constant in the rotating frame ($R_{1\rho}$) measured by spin-locking magnetization along an effective field [4,5]. Theoretical descriptions of these techniques are bountiful in the NMR literature, but the Bloch-McConnell equations [6,7] are probably most often used to describe the evolution of exchanging magnetization. Analytical expressions obtained from the Bloch-McConnell equations typically have complex form. As a result, approximate expressions are more often used to analyze experimental data. Consider, for example, a simple two-site exchange reaction at equilibrium

$$A \underset{k_b}{\overset{k_a}{\rightleftharpoons}} B.$$

The chemical-exchange rate constant for this reaction can be written as

$$k_{ex} = k_a + k_b = k_a/p_b = k_b/p_a,$$

where p_a and p_b are normalized equilibrium populations ($p_a + p_b = 1$) at magnetic sites a and b, respectively. The

* Corresponding author. Fax: +1 612 626 2004.
E-mail address: idiat001@tc.umn.edu (D. Idiyatullin).

1090-7807/$ - see front matter © 2004 Elsevier Inc. All rights reserved.
doi:10.1016/j.jmr.2004.09.008

chemical-shift difference between sites is $\delta\omega = |\omega_a - \omega_b|$. Approximate analytical expressions commonly used to analyze exchange-induced effects on relaxation are given in Eqs. (1)–(5) below.

For a CPMG experiment in the fast-exchange limit ($k_{ex} \gg \delta\omega$), the transverse relaxation rate constant is given by [8]

$$R_{2,ex} = (p_a p_b \delta\omega^2/k_{ex})\left[1 - \tanh\left(k_{ex}\tau_{cp}/2\right)/\left(k_{ex}\tau_{cp}/2\right)\right], \quad (1)$$

where τ_{cp} is the time between centers of 180° pulses of length $T_p \ll \tau_{cp}$. Under the condition $p_a \gg p_b$, an alternative expression describing relaxation at site a for all time scales is [9]

$$R_{2,ex} = p_a p_b \delta^2 k_{ex} \Bigg/ \left[k_{ex}^2 + \sqrt{\left(\left(2\sqrt{3}/\tau_{cp}\right)^4 + p_a^2\delta\omega^4\right)}\right]. \quad (2)$$

On the other hand, the relaxation rate constant in the slow-exchange regime ($k_{ex} \ll \delta\omega$) at site a for $p_a \geqslant p_b$ follows [10,11]

$$R_{2,ex} = k_a\left[1 - \sin\left(\delta\omega\tau_{cp}/2\right)/\left(\delta\omega\tau_{cp}/2\right)\right]. \quad (3)$$

In a conventional spin-lock experiment, magnetization decays along an effective field, $\omega_{eff} = \sqrt{\omega_1^2 + \Delta\omega^2}$, where ω_1 is the amplitude of the RF irradiation (in units of rad/s) and $\Delta\omega$ is the resonance offset defined as the difference between the Larmor frequency and the frequency of the RF irradiation ω_{RF}. In the fast-exchange limit, the rotating frame longitudinal relaxation rate constant can be approximated by [4,5]

$$R_{1\rho,ex} = \sin^2\alpha p_a p_b \delta\omega^2 k_{ex}/\left(\omega_{eff}^2 + k_{ex}^2\right), \quad (4)$$

where $\sin^2\alpha = \omega_1^2/\omega_{eff}^2$ and $\Delta\omega = p_a\omega_a + p_b\omega_b - \omega_{RF}$. Another expression recently proposed to describe $R_{1\rho,ex}$ in the slow-exchange regime with non-equal populations is [12]

$$R_{1\rho,ex} = \sin^2\alpha\ p_a p_b \delta\omega^2 k_{ex}/\left(\omega_{aeff}^2\omega_{beff}^2/\omega_{eff}^2 + k_{ex}^2\right), \quad (5)$$

where $\omega_{aeff} = \sqrt{(\omega_a - \omega_{RF})^2 + \omega_1^2}$ and $\omega_{beff} = \sqrt{(\omega_b - \omega_{RF})^2 + \omega_1^2}$ are the effective fields at sites a and b, respectively.

Unfortunately, Eqs. (1)–(5) offer no possibility to account for changes in experimental conditions. In practice, the agreement between the actual and the estimated relaxation rates depends on multiple experimental factors, particularly those parameters affecting the RF pulses. For example, the observed relaxation rates depend on the length of the pulses in the CPMG train or whether the phase of the spin-lock pulse is modulated in $R_{1\rho}$ experiments. The theoretical description becomes even more complex when the pulse sequence is implemented with shaped pulses having time-dependent amplitudes and phases, as used with adiabatic pulses [13].

Simulations of the influence of chemical exchange on different pulse sequences have been performed using numerical solutions of the system differential equations [14–16]. Among these methods, a preferred approach is based on homogenized Bloch–McConnell equations [16]. However, all of these methods treat the exchange rate as a macroscopic relaxation parameter and are limited to first-order kinetic reactions that can be described by linear differential equations. In principle, by increasing the number and complexity of the differential equations, these methods can be adapted to simulate higher order kinetic reactions. Here, we demonstrate an alternative approach based on a Monte Carlo simulation that treats the chemical-exchange process at the microscopic level. A similar approach has been used to analyze collisional relaxation during neutron transport in solids [17] and ion motion in plasmas [18] and is used in laser chemistry [19,20]. Consideration of relaxation on a microscopic level is the most straightforward way to simulate some complex processes of exchange that occur in actual spin systems. Examples of such cases that come to mind include exchange processes in proteins and peptide solutions that are modulated by cooperative and non-cooperative conformational fluctuations [21–25], a distribution of exchange rates or chemical shifts [26], and the combined effect of exchange and diffusion processes in a magnetic field gradient [27].

The method described below uses a random exchange function in standard product-operator calculations. Results from Monte Carlo simulations of conventional CPMG and $R_{1\rho}$ experiments are presented and compared with predictions from Eqs. (1)–(5). Novel applications of the method are also demonstrated. Specifically, the method is used to simulate the effect of chemical-exchange-induced relaxation during an adiabatic Carr-Purcell (CP) sequence. Finally, simulations are performed to evaluate the effect of a second random process that is superimposed on a simple two-site exchange process in a $R_{1\rho}$ experiment.

2. Method

In the present computational approach, as in the conventional product operator approach, the density matrix $\sigma(t)$ evolves in response to a sequence of events, and between events, the spin Hamiltonian H is time independent [28]. The density matrix at the time when the $(i+1)$th event occurs is

$$\sigma(t_{i+1}) = e^{-iH\Delta t_i}\sigma(t_i)e^{iH\Delta t_i}, \quad (6)$$

where the variable Δt_i is the time separating the ith and $(i+1)$th events. Chemical exchange produces a change in H because spins spontaneously relocate to sites with

different resonance offsets. Here, it is assumed that these exchange events occur instantaneously and can be treated as successive frequency jumps occurring at t_i, t_{i+1}, t_{i+2}... Accordingly, the interval of time between events is variable, and Eq. (6) must be solved successively in time as each change of H takes place. Because exchange is a random process, the complete pulse sequence must be evaluated N times, where N is a statistically large number. To obtain a solution to characterize an ensemble of spins, the average of N spin trajectories must be calculated. One possible trajectory of the density matrix evolution in the presence of the exchange can be described as

$$\sigma_k(t) = \prod \mathrm{e}^{-\mathrm{i}H_i\Delta t_i}\sigma_k(0)\prod \mathrm{e}^{\mathrm{i}H_i\Delta t_i}. \tag{7}$$

The time-independent Hamiltonian during an interval Δt_i is

$$H_i = H_i' + \Delta\omega_i I_z. \tag{8}$$

where H_i' describes the RF irradiation, in addition to other types of spin interactions (e.g., scalar coupling), and $\Delta\omega_i$ is the resonance offset during this particular interval. The full density matrix is simulated by calculating the N random evolution trajectories and obtaining the result as an average of the evolution of the spin system,

$$\sigma(t) = \sum_{k=1}^{N}\sigma_k(t)/N. \tag{9}$$

Subsequently, the exchange contribution is calculated from

$$R_{\mathrm{ex}} = \ln(I_0/I)/T_{\mathrm{seq}}, \tag{10}$$

where T_{seq} is the pulse sequence duration, I and I_0 are amplitudes of some component of the density matrix at the end of the pulse sequence with and without the presence of the chemical exchange process, respectively. Depending on the type of pulse sequence, I and I_0 represent basic operators $I^a_{x,y,z}, I^b_{x,y,z}, I^a_{x,y,z} + I^b_{x,y,z}$ or any kind of zero or n quantum coherences. For the case in which the relaxation process is not described by a simple exponential function, the time dependence of amplitude I can be analyzed.

The central idea of the computational method is straightforward. An important aspect of the method is the procedure used to create a random interval between jumps for simulating the exchange process. For a process with correlation time τ_{ex} ($=1/k_{\mathrm{ex}}$), we assume the probability $P(\Delta t)$ of the following interval between two jumps being Δt depends exponentially according to $P(\Delta t) \sim \mathrm{e}^{-\Delta t/\tau_{\mathrm{ex}}}$. A computer generates a random number $y \in [0,1]$ having uniform distribution. Using this random number, a random time interval $\Delta t \in [0,\infty]$ with a normalized exponential distribution $P(\Delta t) = \mathrm{e}^{-\Delta t/\tau_{\mathrm{ex}}}/\tau_{\mathrm{ex}}$ can be obtained by solving the equation [17]

$$\int_0^{\Delta t} P(x)\mathrm{d}x = y. \tag{11}$$

As a result, with y distributed uniformly, an exponentially-distributed random time interval is obtained from

$$\Delta t = -\tau_{\mathrm{ex}}\ln(1-y). \tag{12}$$

To simulate different populations of sites, the value of τ_{ex} in Eq. (12) can simply be varied for the different sites as $\tau^i_{\mathrm{ex}} = \tau_{\mathrm{ex}}/p_i$. Although only the two-site exchange case is considered here, the method can be readily generalized to other cases. The protocol of simulation each trajectory in the case of n sites should include: (i) randomly choosing the starting site, (ii) randomly seeking the site dependent interval Δt, and (iii) randomly choosing the site of destination after every jump. Steps (ii) and (iii) are repeated until $T_{seq} = \sum \Delta t_i$. Possible modifications of this protocol to permit adaptation to more complex cases are briefly mentioned here. (a) *A distribution of the exchange rates*: any expected distribution function can be considered by simple modification of the Eq. (12) for generating the site dependent interval Δt. (b) *A distribution of chemical shifts of the exchangeable sites*: this case can be simulated as an n site case with distributed probability of sites. (c) *Diffusion of the exchangeable sites in a magnetic field gradient*. This case can be realized by including in (ii) the random walk process in the presence of a magnetic field gradient, which works simultaneously and independently from the site exchange process. The instantaneous product operator calculation must use the sum of chemical exchange and space dependent frequency shift values. (d) *The modulation of chemical exchange process by another random process*. This case can be simulated in two different ways: (1) by increasing the number of exchangeable sites or (2) by directly including another random process which changes the properties of the sites. For example, consider a two-site (p_{a} and p_{b}) exchange process which can go faster or slower, with dependency on another random process having two probabilities p_{o} and p_{c}. This case describes the four site exchange process with probabilities: $p_{\mathrm{o}}p_{\mathrm{a}}$, $p_{\mathrm{o}}p_{\mathrm{b}}$, $p_{\mathrm{c}}p_{\mathrm{a}}$, and $p_{\mathrm{c}}p_{\mathrm{b}}$. An alternative way is to include another simultaneous and independent process that changes the exchange rates. The results of simulation performed in this latter manner are presented later.

A procedure to estimate the accuracy of the final result is an essential component of any simulation method. The standard deviation ΔR_{ex} depends on the value of the ratio I_0/I and on parameters N, T_{seq}, and τ_{ex} [29]. The necessary number of repetitions N cannot be estimated before performing a simulation because I_0/I is unknown and is a nonlinear function of τ_{ex}. The approach used here is equivalent to that usually practiced in Monte Carlo simulations [29]. Specifically, q separate simulations are performed to obtain q unique estimates of

the relaxation rate constant R_{ex}^{i}. After finding the average, $\overline{R}_{ex} = \sum R_{ex}^{i}/q$, the standard deviation is calculated from $\Delta R_{ex} = \sqrt{\frac{\sum (R_{ex}^{i} - \overline{R}_{ex})^2}{q}}$. The simulation is repeated with increasing N until $\Delta R_{ex}/\overline{R}_{ex}$ reaches the required upper limit. In the present work, the estimated precision of the simulations was better than 5% ($\Delta R_{ex}/\overline{R}_{ex} < 0.05$) using $q = 10$. Because precision was fixed, the time required to obtain a single data point varied from 0.1 to 100 point/s when using a computer with a 3 GHz processor.

3. Simulation results

3.1. The CPMG experiment

The CPMG pulse sequence can be written as $90^{\circ}_{y} - (\tau_{cp}/2 - 180^{0}_{x} - \tau_{cp}/2)_{m}$, where m is the echo number. In this case, I and I_0 represent the operators $I_x^a + I_x^b$. Fig. 1 shows $R_{2,ex}$ data plotted as a function of k_{ex} for a CPMG experiment using $p_a = p_b$ and $\delta\omega/2\pi = 100$ Hz, for two different τ_{cp} values. The data shown describe CPMG experiments performed with ideal 180° pulses ($T_p \ll \tau_{cp}$) using either the first or 12th echo. With these parameters, Eqs. (1)–(3) predict the same $R_{2,ex}$ data in the slow-exchange regime. In the intermediate and fast-exchange regimes, Eq. (2) gives a slightly bigger value of $R_{2,ex}$ than that predicted by Eq. (1). In this region, greatest precision is expected with Eq. (1), because Eq. (3) describes only slow exchange and the application of Eq. (2) is incompatible with the condition $p_a = p_b$. Simulated data generated for the 12th echo ($m = 12$) show good agreement with Eq. (1) over a broad range of $R_{2,ex}$ and k_{ex} values. Such good agreement between theory and simulation is supporting evidence of the robustness of our computational method. For the case of the first echo, plots in Fig. 1 reveal significant disagreement between simulated data and theoretical expectations (Eq. (1)). Interestingly, the discord between theory and simulation observed in this case ($m = 1$) is consistent with the theoretical expectation of the existence of a faster second pseudo-exponential term [30]. Understanding the non-exponential decay in CPMG experiments is important for studies of fast relaxing spins (e.g., large proteins) which must be performed with small m to minimize signal loss [31]. According to Fig. 1, the non-exponential behavior reaches a maximum when $k_{ex}\tau_{cp} \approx 2\sqrt{3}$ and becomes negligible approximately in the range of $\sqrt{3}/5 > k_{ex}\tau_{cp} > 20\sqrt{3}$. These features characterize not only the simulations shown (Fig. 1), but also data obtained from CPMG simulations using other values of τ_{cp} (data not shown). To further demonstrate the dependence on echo number, Fig. 2 shows $R_{2,ex}$ data plotted as function of m, for the case of $k_{ex}\tau_{cp} = 2\sqrt{3}$. Interestingly, when using $m = 1$, the simulated value of $R_{2,ex}$ deviates by as much as 25% from theoretical value (Eq. (1)). As can be seen from Fig. 2, accuracy better than 5% can be reached by performing measurements with $m > 5$.

In the slow-exchange regime, the simulation method was used to investigate the $R_{2,ex}$ dependence on the CPMG field strength, $v_{cp} = 1/2\tau_{cp}$. In this case, the operator of interest is I_x^a (for site a only). Fig. 3 shows $R_{2,ex}$ data plotted as a function of v_{cp}, for the cases of $m = 1$ and 12, and separately for $p_b = p_a$ and $p_b \neq p_a$ cases.

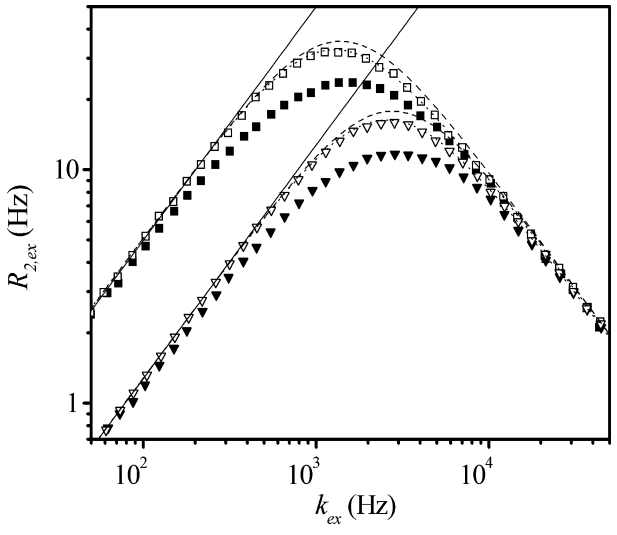

Fig. 1. The $R_{2,ex}$ dependency on k_{ex} for CPMG experiments, as predicted by simulations (symbols) or theoretically from Eqs. (1)–(3) (dotted, dashed, and solid lines, respectively). The calculations assumed ideal 180° pulses ($T_p \ll \tau_{cp}$), $p_a = 0.5$, $\delta\omega/2\pi = 100$ Hz, and two different values of τ_{cp}: 2.5 ms (square) and 1.25 (triangle). Simulations were carried on the first (solid symbol) and twelfth (open symbol) echo.

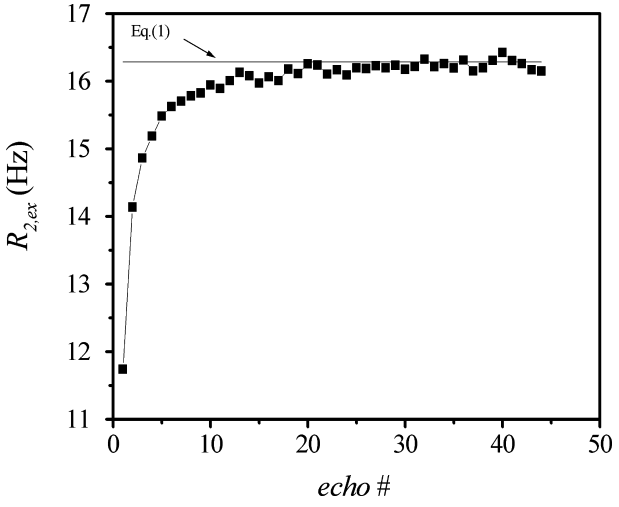

Fig. 2. The $R_{2,ex}$ dependence on echo number m. Calculations were performed with $\delta\omega/2\pi = 100$ Hz, $p_a = 0.5$, $\tau_{cp} = 1.25$ ms, and $k_{ex} = 2\sqrt{3}/\tau_{cp}$.

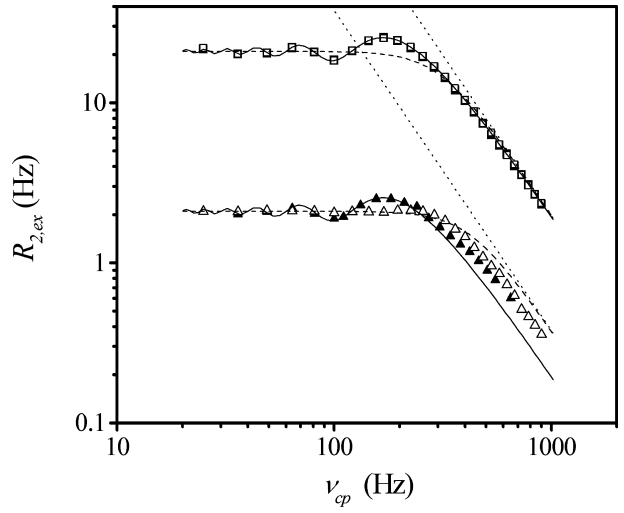

Fig. 3. The $R_{2,\mathrm{ex}}$ dependence on the CPMG field strength $\nu_{\mathrm{cp}} = 1/2\tau_{\mathrm{cp}}$, for two different populations, $p_{\mathrm{a}} = 0.5$ (square) and $p_{\mathrm{a}} = 0.95$ (triangle). Other parameters were: $\delta\omega/2\pi = 480$ Hz and $k_{\mathrm{ex}} = 42$ Hz. The data for the first (solid symbol) and twelfth (open symbol) echo are shown. Dotted, dashed, and solid lines correspond to the theoretical predictions of Eqs. (1)–(3), respectively.

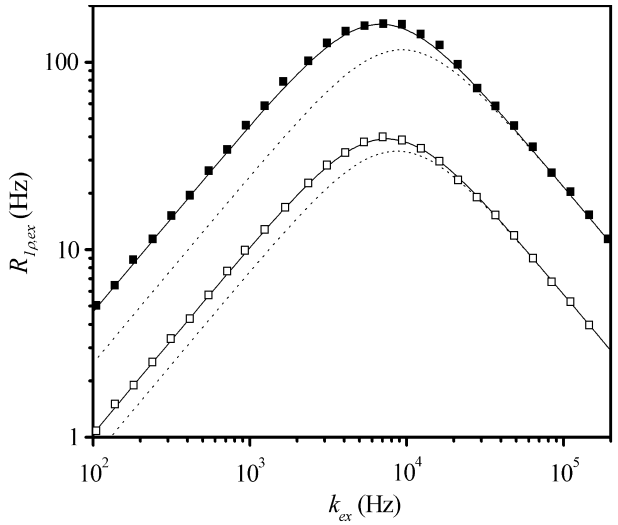

Fig. 4. The $R_{1\rho,\mathrm{ex}}$ dependence on k_{ex} for off resonance experiments with $p_{\mathrm{a}} = 0.75$ for $\delta\omega/2\pi = 1000$ Hz (solid) and $\delta\omega/2\pi = 480$ Hz (open). Dotted and solid curves were calculated theoretically using Eqs. (4) and (5), respectively.

According to theory [11], in the low end of the ν_{cp} range, $R_{2,\mathrm{ex}}$ oscillates and has an amplitude scaled linearly to $k_{\mathrm{a}} = k_{\mathrm{ex}}p_{\mathrm{b}}$, with a tendency to extrapolate to k_{a} as $\nu_{\mathrm{cp}} \to 0$. The asymptotes of these dependencies are described well by Eq. (2). For the case of $p_{\mathrm{b}} = p_{\mathrm{a}}$, the simulations results are identical for $m = 1$ and $m = 12$ and perfectly agree with Eq. (3). However, for the case $p_{\mathrm{b}} \neq p_{\mathrm{a}}$ and large m, Eq. (2) provides the best descriptions of the simulation results, whereas Eq. (1) also yields close agreement in the high CPMG field strength limit ($\delta\omega < \nu_{\mathrm{cp}}$). According to these and other simulations conducted under different conditions (data not shown), Eq. (1) appears to be applicable over a much wider range of exchange time scales than those predicted by theory and can be applied to all values of k_{ex} provided the condition $\delta\omega < \nu_{\mathrm{cp}}$ is satisfied.

3.2. Off-resonance $R_{1\rho}$ experiments

A convenient pulse sequence used for off-resonance $R_{1\rho}$ measurement can be written as $\mathrm{Ad}^{+} - \mathrm{spin\ lock}_x - \mathrm{Ad}^{-}$, where Ad^{+} and Ad^{-} are adiabatic passage pulses used to rotate magnetization by angle α for spin-locking and to rotate the magnetization back to the longitudinal axis after the spin-lock pulse, respectively [32]. In this case, I and I_0 represent the operators $I_z^a + I_z^b$. To avoid any effects from Ad^{+} and Ad^{-}, in the calculations these pulses were assumed to perform ideal transformations: $I_z \to I_z \sin\alpha + I_y \cos\alpha$ and $I_z \sin\alpha + I_y \cos\alpha \to I_z$, respectively.

Fig. 4 shows off-resonance $R_{1\rho,\mathrm{ex}}$ values plotted as a function of k_{ex} for the case of $p_{\mathrm{a}} = 0.75$ with two different values of $\delta\omega$. The $R_{1\rho,\mathrm{ex}}$ values obtained by simulation are in excellent agreement with the curves generated with Eq. (5) over the complete range of time scales, whereas the curve predicted by Eq. (4) deviates considerably in the slow exchange regime. Furthermore, significant disagreement between data generated with Eq. (4) versus Eq. (5) and the simulated data remains as $\delta\omega$ and $\Delta\omega$ vary, as shown in Fig. 5. To the best of our knowledge the experimental verification of the Eq. (5) has been reported only once before [33]. Although a previous report [12] already demonstrated excellent agreement between Eq. (5) and simulations based on Bloch-McConnell equations, the simulation results obtained here using the alternative Monte Carlo approach can

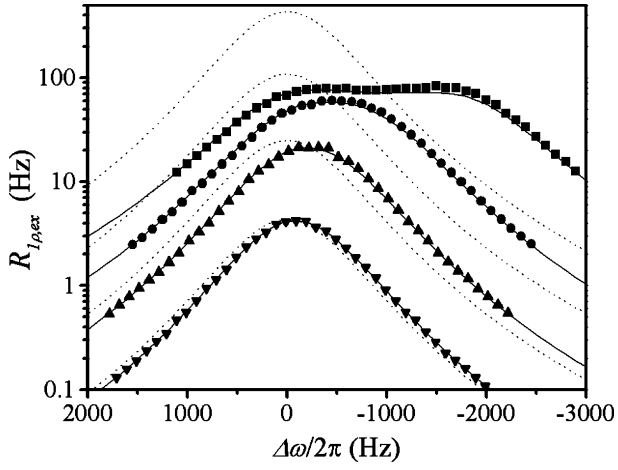

Fig. 5. The offset dependence of $R_{1\rho,\mathrm{ex}}$ using $\delta\omega/2\pi = 2000$ Hz (square), 1000 Hz (circle), 480 Hz (up triangle), and 200 Hz (down triangle). Other parameters were: $p_{\mathrm{a}} = 0.95$, $k_{\mathrm{ex}} = 1638$ Hz, and $\omega_1/2\pi = 805$ Hz. Dotted and solid curves were calculated theoretically using equation Eqs. (4) and (5), respectively.

be considered as further evidence for the validity of Eq. (5).

3.3. The adiabatic Carr-Purcell experiment

The next experiment considered here is the adiabatic CP pulse sequence, $90^{\circ}_{y} - (\mathrm{HS1}_{x} - \mathrm{HS1}_{x} - \mathrm{HS1}_{-x} - \mathrm{HS1}_{-x})_{m}$, where HS1 denotes a hyperbolic secant pulse [34]. Each HS1 pulse performs an adiabatic full-passage (180°) of duration T_{p}. The amplitude and frequency modulated functions for the HS1 pulse [35] are given by

$$\omega_1(t) = \omega_1^{\max}\mathrm{sech}(\beta\tau), \tag{13}$$

$$\omega_{\mathrm{RF}}(t) = \omega_{\mathrm{c}} + A\tanh(\beta\tau), \tag{14}$$

where ω_{c} is the carrier frequency, β is a truncation factor ($\mathrm{sech}\,\beta = 0.01$), τ is normalized time ($=2t/T_{\mathrm{p}} - 1$), A is the amplitude of the frequency sweep, and $\omega_1^{\max}$ is the maximum value of $\omega_1(t)$. The simulated data is compared with theoretical estimation of the exchange contribution during each HS1 pulse as described below. For simplicity, the case considered is

$$A = \omega_1^{\max}, \tag{15}$$

for the on-resonance condition ($\omega_{\mathrm{o}} = \omega_{\mathrm{c}}$). Accordingly, the amplitude of effective field ω_{eff} during the HS1 pulse remains constant ($\omega_{\mathrm{eff}} = A = \omega_1^{\max}$). Two approximations are used in the calculations. First, the vector of ω_{eff} remains orthogonal to the magnetization vector during the pulse [13], which results in transverse relaxation in the rotating frame $R_{2\rho,\mathrm{ex}}$ about the time-dependent direction of ω_{eff} [34]. Second, for estimation of $R_{2\rho,\mathrm{ex}}$ the approximate expression in the fast exchange limit is used [34]

$$R_{2\rho,\mathrm{ex}} = R_{2,\mathrm{ex}}\cos^2\alpha. \tag{16}$$

In these approximations, the average exchange contribution to relaxation during adiabatic pulse can be obtained as

$$\overline{R}_{2\rho,\mathrm{ex}} = \frac{R_{2,\mathrm{ex}}}{T_{\mathrm{p}}}\int_0^{T_{\mathrm{p}}}\cos^2\alpha(t)\mathrm{d}t. \tag{17}$$

Using Eqs. (13) and (14) to describe $\alpha(t)$, for HS1 the expression becomes

$$\overline{R}_{2\rho,\mathrm{ex}} = \frac{R_{2,\mathrm{ex}}(\beta - 1)}{\beta}. \tag{18}$$

Fig. 6 shows $\overline{R}_{2\rho,\mathrm{ex}}$ values plotted as a function of k_{ex} for the cases of $p_{\mathrm{a}} = 0.5$ using five different values of T_{p}. The solid lines represent the theoretical predictions based on Eq. (18) with $R_{2,\mathrm{ex}}$ values calculated according to Eq. (1). Peak RF amplitude was chosen as $\omega_1^{\max} = 20\pi/T_{\mathrm{p}}$ to satisfy the condition of Eq. (15). The theoretical approximation (Eq. (18)) describes the simulated data within ~10% accuracy over the full range of k_{ex} values. As was shown previously [34], an advantage of the adiabatic CP pulse sequence is the ability to modulate the influence of chemical exchange on relaxation rates by adjusting pulse parameters (e.g., $\omega_1^{\max}$, A, T_{p}, and modulation functions).

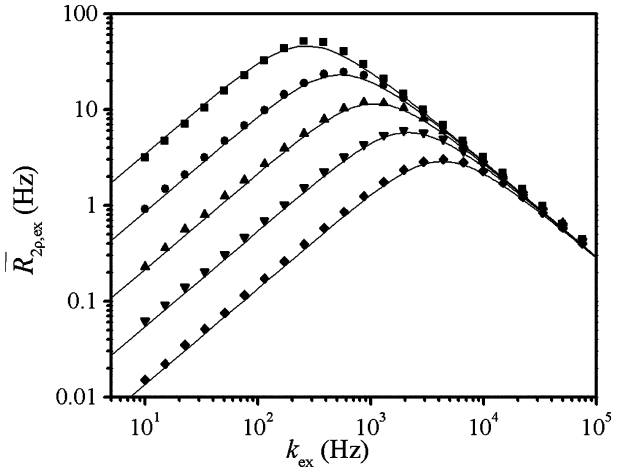

Fig. 6. The dependence of exchange contribution during adiabatic CP pulse sequence $\overline{R}_{2\rho,\mathrm{ex}}$ on k_{ex} for the five different values of T_{p}: 12 ms (square), 6 ms (circle), 3 ms (up triangle), 1.5 ms (down triangle), and 0.75 ms (diamond). Other parameters: $p_{\mathrm{a}} = 0.5$, $\delta\omega/2\pi = 60$ Hz, $\omega_1^{\max}/2\pi = 10/T_{\mathrm{p}}$. The theoretical approximations were calculated by using Eq. (18) with $R_{2,\mathrm{ex}}$ values calculated according to Eq. (1).

3.4. Chemical exchange modulated by a second random process during a $R_{1\rho}$ experiment

In systems such as proteins or peptide solutions, a two-site chemical exchange model is often an oversimplification of the actual molecular dynamics. The exchange parameters such as kinetic rates and chemical-shift values depend on conformational dynamics. Here, simulations are performed for the case in which a second random process, that originating in conformational dynamics, modulates the two-site chemical exchange process.

For simplicity, the two sites are assumed to have equal populations (p_{a} and p_{b}). In contrast to the previous simulations above, the present simulation uses two independent random time-interval generators. For the purpose of demonstration, the second random process is also chosen to have equal populations (p_{o} and p_{c}) or correlation times (τ_{o} and τ_{c}), with modulation frequency given by $k_{\mathrm{m}} = 1/p_{\mathrm{o}}\tau_{\mathrm{c}} = 1/p_{\mathrm{c}}\tau_{\mathrm{o}}$. Indexes o and c are used to denote conformational states characterized by less and more hindrance (open and closed) to the exchange process. The simple case chosen for consideration here is $k_{\mathrm{ex}} = k_{\mathrm{a}} + k_{\mathrm{b}}$ for state o and $k_{\mathrm{ex}} = 0$ for state c. Fig. 7 shows on-resonance $R_{1\rho,\mathrm{ex}}$ values plotted as a function of k_{ex} for different values of k_{m}. For comparison, the plotted lines in the figure depict the expected values of $R_{1\rho,\mathrm{ex}}(k_{\mathrm{ex}}/2)$ (solid line) and $0.5R_{1\rho,\ \mathrm{ex}}$ (k_{ex}) (dash line), obtained from Eq. (4) for $p_{\mathrm{o}} = 1$ (always open).

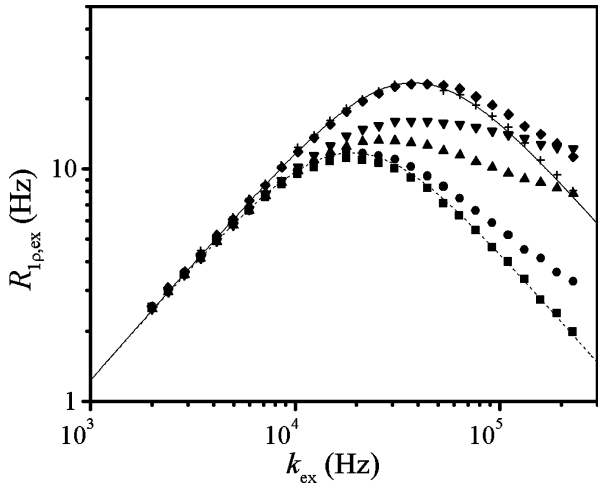

Fig. 7. The on-resonance $R_{1\rho,\mathrm{ex}}$ values plotted as a function of k_{ex} in the presence of an exchange modulation process with $p_o = p_c$ for six different values of k_m, which are: 0.1 Hz (square), 1 kHz (circle), 5 kHz (up triangle), 10 kHz (down triangle), 100 kHz (diamond), and 1000 kHz (cross). The lines are calculated (Eq. (4)) values of $R_{1\rho,\mathrm{ex}}(k_{\mathrm{ex}}/2)$ (solid line) and $0.5R_{1\rho,\mathrm{ex}}(k_{\mathrm{ex}})$ (dash line) for $p_o = 1$ always open case. Other parameters: $p_a = 0.5$, $\delta\omega/2\pi = 300$ Hz $\delta_1/2\pi = 3000$ Hz.

According to Fig. 7 these two cases agree with simulation data for the two limiting cases: $k_{\mathrm{ex}} \ll k_m$ and $k_{\mathrm{ex}} \gg k_m$, respectively. These agreements are to be expected. The fast modulation process in the $p_o = p_c$ case acts as a probability factor decreasing the chemical-exchange rate by a factor of two. Alternatively, if the modulation process is very slow, the system can be considered as a sum of o and c states existing independently. As a consequence of this, in the slow modulation regime nonexponential behavior of relaxation decay is observed. The behavior of $R_{1\rho,\mathrm{ex}}(k_{\mathrm{ex}})$ in the intermediate regime depends on many factors including pulse sequence parameters. These simulation results demonstrate how a second random process can have a significant non-linear effect on relaxation rates, although experimental verification of these findings is needed.

4. Conclusions

A method has been described to simulate the effects of chemical exchange on relaxation. The approach is based on the inclusion of a random exchange process in product operator calculations on a microscopic level. As compared with other simulation methods that are based on the full analysis of the system of Bloch-McConnell equations [14–16], this alternative method has the advantage of simplicity and can be easily adapted to evaluate spin dynamics in highly complex systems. Here, it was shown that the method can be used to evaluate existing theoretical approximations and to predict exchange-induced relaxation rates when using complex pulse sequences. As shown, the method seizes all ranges of the time scale of exchange measurable by NMR. The consideration of the exchange process on the microscopic level allows straightforward inclusion of such effects as the distribution of kinetic rates and chemical shifts, diffusion in an inhomogeneous magnetic field, and modulation of the exchange by other random processes. The described method is included as a subprogram in NMRKITCHEN which is available via Internet at www.cmrr.umn.edu.

Acknowledgments

The authors are grateful to the Dr. Elena Ermakova (Kazan Institute of Biochemistry and Biophysics), for the useful discussion. This research was supported by NIH Grants P41 RR08079 and RO1 CA92004.

References

[1] A.G. Palmer Iii, C. Kroenke, J. Loria, Nuclear magnetic resonance methods for quantifying microsecond-to-millisecond motions in biological macromolecules, Methods Enzymol. 339 (2001) 204–238.
[2] H. Carr, E. Purcell, Effect of diffusion on free precession in nuclear magnetic resonance experiments, Phys. Rev. 94 (1954) 630–638.
[3] S. Meiboom, D. Gill, Modified spin-echo method for measuring nuclear relaxation times, Rev. Sci. Instrum. 29 (1958) 688–691.
[4] C. Deverell, R. Morgan, J. Strange, Studies of chemical exchange by nuclear magnetic relaxation in the rotating frame, Mol. Phys. 18 (1970) 553–559.
[5] H. Desvaux, P. Berthault, Study of dynamic processes in liquids using off-resonance rf irradiation, Prog. Nucl. Magn. Reson. Spectrosc. 35 (1999) 295–340.
[6] H.M. Mcconnell, Reaction rates by nuclear magnetic resonance, J. Chem. Phys. 28 (1958) 430–431.
[7] J. Cavanagh, W.J. Fairbrother, A.G. Palmer, N.J. Skelton, Protein NMR Spectroscopy, Academic Press, San Diego, 1996.
[8] Z. Luz, S. Meiboom, Nuclear magnetic resonance study of the photolysis of trimethylammonium ion in aquous solution-order of the reaction with respect to solvent, J. Chem. Phys. 39 (1963) 366–370.
[9] R. Ishima, D.A. Torchia, Estimating the time scale of chemical exchange of proteins from measurements of transverse relaxation rates in solution, J. Biomol. NMR 14 (1999) 369–372.
[10] H.S. Gutowsky, R.L. Vold, E.J. Wells, Theory of chemical exchange effects in magnetic resonance, J. Chem. Phys. 43 (1965) 4107–4125.
[11] M. Tollinger, N.R. Skrynnikov, F.A.A. Mulder, J.D. Forman-Kay, L.E. Kay, Slow dynamics in folded and unfolded states of an SH3 domain, J. Am. Chem. Soc. 123 (2001) 11341–11352.
[12] O. Trott, A.G. Palmer, R_{1r} relaxation outside the fast-exchange limit, J. Magn. Reson. 154 (2002) 157–160.
[13] M. Garwood, L. DelaBarre, The return of the frequency sweep: designing adiabatic pulses for contemporary NMR, J. Magn. Reson. 153 (2001) 155–177.
[14] M. Cuperlovic, G.H. Meresi, W.E. Palke, J.T. Gerig, Spin relaxation and chemical exchange in NMR simulations, J. Magn. Reson. 142 (2000) 11–23.

[15] R.S. Dumont, S. Jain, A. Bain, Simulation of many-spin system dynamics via sparse matrix methodology, J. Chem. Phys. 106 (1997) 5928–5936.
[16] M. Helgstrand, T. Härd, P. Allard, Simulations of NMR pulse sequences during equilibrium and non-equilibrium chemical exchange, J. Biomol. NMR 18 (2000) 49–63.
[17] J. Spanier, E.M. Gelbard, Monte Carlo Principles and Neutron Transport Problems, Addison-Wesley, Reading, MA, 1969, p. 234.
[18] S.L. Lin, J.N. Bardsley, Monte Carlo simulation of ion motion in drift tubes, J. Chem. Phys. 66 (1977) 435–445.
[19] S. Longo, D. Bruno, M. Capitelli, P. Minelli, A Monte Carlo model for the non-equilibrium coherent kinetics of ensembles of two level systems, Chem. Phys. Lett. 316 (2000) 311–317.
[20] S. Longo, D. Bruno, P. Minelli, Direct simulation of non-linear interparticle collisional relaxation of ensembles of two-level systems, Chem. Phys. 256 (2000) 265–273.
[21] K.-S. Kim, C.K. Woodward, Protein internal flexibility and global stability: effect of urea on hydrogen exchange rates of bovine pancreatic trypsin inhibitor, Biochemistry 32 (1993) 9609–9613.
[22] N.A. Farrow, J.R. Muhandham, A.U. Singer, S.M. Pascal, C.M. Kay, G. Gish, S.E. Shoelson, T. Pawson, J.D. Forman-Kay, L.E. Kay, Backbone dynamics of a free and a phosphopeptide-complexed src homology 2 domain studied by ^{15}N NMR relaxation, Biochemistry 33 (1994) 5984–6003.
[23] E.Z. Eisenmesser, D.A. Bosco, M. Akke, D. Kern, Enzyme dynamics during catalysis, Science 295 (2002) 1520–1523.
[24] M. Ottiger, O. Zerbe, P. Guntert, K. Wuthrich, The NMR solution conformation of unligated human cyclophilin A, J. Mol. Biol. 272 (1997) 64–81.
[25] D. Kern, G. Kern, G. Scherer, G. Fischer, T. Drakenbergs, Kinetic analysis of cyclophilin-catalyzed prolyl cis-trans isomerization by dynamic NMR spectroscopy, Biochemistry 34 (1995) 13594–13602.
[26] J.M. Schurr, B.S. Fujimoto, R. Diaz, B.H. Robinson, Manifestations of slow site exchange processes in solution NMR: a continuous Gaussian exchange model, J. Magn. Reson. 140 (1999) 404–431.
[27] Y. Gossuin, A. Roch, R. Muller, P. Gillis, An evaluation of the contributions of diffusion and exchange in relaxation enhancement by MRI contrast agents, J. Magn. Reson. 158 (2002) 36–42.
[28] R. Ernst, G. Bobenhausen, A. Wokaun, Principles of Nuclear Magnetic Resonance in One and Two Dimensions, Clarendon Press, Oxford, 1997, p. 518.
[29] A.R. Leach, Molecular Modelling: Principles and Applications, Person Education, Harlow, England, 2001, p. 744.
[30] A. Allerhand, H.S. Gutowsky, Spin-echo studies of chemical exchange. II. Closed formulas for two sites, J. Chem. Phys. 42 (1965) 1587–1599.
[31] C. Wang, A.G. Palmer, Solution NMR methods for quantitative identification of chemical exchange in ^{15}N-labeled proteins, Magn. Reson. Chem. 41 (2003) 866–876.
[32] F.A.A. Mulder, R.A. Graaf, R. Kaptein, R. Boelens, Off-resonance rotating frame relaxation experiment for the investigation of macromolecular dynamics using adiabatic rotations, J. Magn. Reson. 131 (1998) 351–357.
[33] D.M. Korzhnev, V.Y. Orekhov, F.W. Dahlquist, L.E. Kay, Off-resonance R_{1r} relaxation outside of the fast exchange limit: an experimental study of a cavity mutant of t4 lysozyme, J. Biomol. NMR 26 (2003) 39–48.
[34] S. Michaeli, D.J. Sorce, D. Idiyatullin, K. Ugurbil, M. Garwood, Transverse relaxation in the rotating frame induced by chemical exchange, J. Magn. Reson. 169 (2004) 293–299.
[35] M.S. Silver, R.I. Joseph, D.I. Hoult, Selective spin inversion in nuclear magnetic resonance and coherent optics through an exact solution of the Bloch- Riccati equation, Phys. Rev. A 31 (1985) 2753–2755.